Characterization of Photoinduced Electron Transfer in Jet-Formed Acceptor Donor Complexes. 2. Photoinduced Electron Transfer: Rates and Mechanisms

A. Tramer,[†] V. Brenner,[‡] P. Millié,[‡] and F. Piuzzi*[,‡]

CNRS Laboratoire de Photophysique Moléculaire Bat. 213, Université Paris Sud, 91405 Orsay cedex, France, and CEA-CEN Saclay DRECAM-SPAM Bat. 522, 91191 Gif sur Yvette cedex, France

Received: October 21, 1997; In Final Form: December 19, 1997

The electron transfer (ET) rates induced by the electronic excitation of different isomers of anthracene complexes with aniline derivatives are deduced from their fluorescence and fluorescence excitation spectra. The shapes of potential energy surfaces of locally excited and ionic surfaces are calculated with a special interest for the crossing areas of both surfaces. The dependence of the ET rates on the initial configuration is discussed and the assignments of calculated configurations to isomeric species (E and R isomers) are proposed.

I. Introduction

In the first part of this work (further denoted as part 1), we identified a number of isomeric forms for each of anthracene complexes with dimethylaniline and some of its derivatives. The characteristic feature of this group of molecular systems, extensively studied in solutions,[1,2] is the electron transfer (ET) from the locally excited state A* + D (or A*D) to the ionic state A^-D^+, where A is the electron acceptor (anthracene in our case) and D is the electron donor (aniline derivative). Similar systems have been studied by other authors.[3−5] The scope of the present paper is to elucidate the relationship between the structure of an isomer and essential parameters of ET in an isolated jet cooled complex.

We will present: (i) the outlines of the theoretical model for description of ET in isolated molecules (for a more detailed treatment see reference 6), (ii) the summary of experimental data relevant for elucidation of ET processes, (iii) the calculation of excited-state potential energy surfaces and the estimation of the inter-state coupling strength, and (iv) an attempt to assign a calculated configuration to an observed isomeric species.

II. Simplified Theoretical Treatment of the Electron Transfer in Isolated Molecular Systems

We will consider three diabatic electronic states (eigenstates of the zero-order Hamiltonian H^0): the ground g-state AD, the locally excited (LE) state A*D, and the ionic (ion) state A^-D^+. As in usual van der Waals complexes, the g and LE states are weakly bound with nearly the same bonding energies and similar equilibrium configurations $Q_g \approx Q_{LE}$. Specific properties of exciplexes are due to an interaction between the LE state and the closely lying ionic state with the equilibrium configuration $Q_{ion} \neq Q_{LE}$ corresponding to a strongly reduced mean D−A distance. The potential energy minimum of the ionic state $V_{ion}(Q_{ion})$ is deeper than that of the LE state $V_{LE}(Q_{LE})$, but in the $Q \approx Q_{LE} \approx Q_g$ range, $V_{ion}(Q) > V_{LE}(Q)$, so that potential energy surfaces of LE and ionic states cross at Q_c intermediate between Q_{LE} and Q_{ion} (Figure 1). These zeroth-order (diabatic) states are coupled with a configuration dependent coupling matrix element $H_{LE,ion}(Q)$ supposed to be proportional to the overlap integrals S_{AD} between the molecular orbitals involved in the D → A* electron transfer : highest occupied orbitals (HOMO) of the donor and acceptor.

As recently discussed by Jortner et al.[7] and by Deperasinska and Prochorow,[8] the electron-transfer processes in isolated systems may be considered as a specific case of nonradiative transitions from the LE to the ionic state. Since $Q_{LE} \approx Q_g$, the optical excitation of AD (vertical transition) prepares the LE state from which the electron transfer (i.e., LE → ionic transition) occurs.

This process may also be considered as an evolution of the initially prepared wavepacket at the surface of a single adiabatic state A. The A-state is the lower of the pair of adiabatic states obtained by diagonalization of the hamiltonian in the LE-ion basis. Its wave function $|A\rangle$ is strongly dependent on the configuration of the complex Q:

$$|A(Q)\rangle = a(Q)|LE\rangle + b(Q)|ion\rangle \qquad (1)$$

If $H_{LE,ion}(Q)$ is not very large and varies slowly with Q, $|A(Q)\rangle$ will be nearly identical with $|LE\rangle$ ($a^2 \gg b^2$) for $Q \approx Q_{LE}$ and with $|ion\rangle$ for $Q \approx Q_{ion}$ ($b^2 \gg a^2$). In the same way:

$$V_A(Q_{LE}) \approx V_{LE}(Q_{LE}) \qquad \text{and} \qquad V_A(Q_{ion}) \approx V_{ion}(Q_{ion})$$

In contrast, in the intersection of LE and ionic surfaces $V_{LE}(Q_c) = V_{ion}(Q_c)$ so that $a^2 = b^2$. For $Q = Q_c$, the potential energy of the A-state is equal to

$$V_A(Q_c) = V_{LE}(Q_c) - |H_{LE,ion}(Q_c)| \qquad (2)$$

and the essential parameter for the treatment of energy transfer at the adiabatic surface is the energy difference ΔV:

$$\Delta V = V_A(Q_c) - V_A(Q_{LE})$$

Since $V_A(Q_{LE}) > V_A(Q_{ion})$, $\Delta V > 0$ corresponds to the existence of two minima at the A-state energy surface separated by an energy barrier (Figure 1a), while for $\Delta V \leq 0$ this surface is barrierless (Figure 1b).

[†] CNRS Laboratoire de Photophysique Moléculaire.
[‡] CEA-CEN Saclay DRECAM-SPAM.

S1089-5639(97)03389-6 CCC: $15.00
Published on Web 04/08/1998

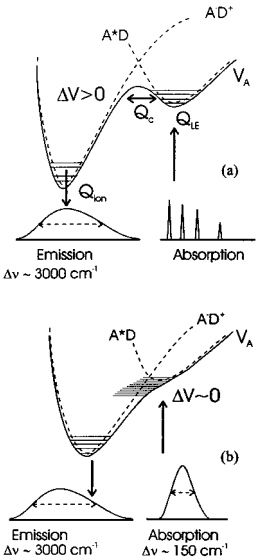

Figure 1. Crossing of LE and ionic potential energy surfaces, shape of the A-state surface and vibrational levels in the case of (a) weak coupling limit and (b) strong coupling as well as shapes of absorption and emission spectra for each case.

In terms of diabatic states, these two cases correspond to (i) $|H_{LE,ion}(Q_c)| < [V_{LE}(Q_c) - V_{LE}(Q_{LE})]$ (defined as the weak coupling case) implies $\Delta V > 0$ and (ii) $|H_{LE,ion}(Q_c)| > [V_{LE}(Q_c) - V_{LE}(Q_{LE})]$ (the strong coupling case) gives $\Delta V \leq 0$.

As already mentioned, the optical excitation prepares the excited system at $Q \approx Q_{LE}$. This process may be described either as the initial excitation of the LE state followed by the electronic relaxation LE ⇝ ion or as a selective excitation of a limited set of the vibronic levels of the A-state (wave packet) followed by the vibrational energy redistribution within the A-state equivalent of an isomerization of the complex from its initial configuration $Q \approx Q_{LE}$ to $Q \approx Q_{ion}$. Since $|A(Q_{LE})\rangle \approx |LE\rangle$ and $|A(Q_{ion}) \approx |ion\rangle$, this isomerization corresponds to the transfer of the electron density from D to A*.

The choice of the basis set depends on the coupling strength in the relevant region of the coordinate space, the adiabatic basis being, as usual, more appropriate in the strong coupling limit.

In the weak coupling limit, we consider two manifolds of interacting levels: a discrete set of low levels of the LE state and a dense manifold of high vibronic levels of the ionic state, coupled by

$$H'_{LE,ion} = H_{LE,ion}(Q_c)\mathrm{AFC}(\upsilon_{LE}) \qquad (3)$$

where $\mathrm{AFC}(\upsilon_{LE})$ is the averaged Franck−Condon factor for initially excited level of the LE state.[7] The ET rate is then given by the Fermi golden rule

$$k_{ET}(\upsilon_{LE}) = (2\pi/h)(H'_{LE,\,ion})^2\rho_{ion} \qquad (4)$$

where ρ_{ion} is the density of levels of the final (ionic) state. Since the electronic coupling matrix element $H_{LE,ion}$ does not depend on υ_{LE} (i.e., on the vibrational energy E_{vib} of the initially excited level) and the $(H_{LE,ion})^2\rho_{ion}$ term varies slowly with $E_{vib,}$ the dependence of k_{ET} on E_{vib} is determined by the shape of the AFC $= f(E_{vib})$ dependence. One can easily show that AFC increases with E_{vib} and attains its maximum for $E_{vib} = \Delta V$ but for the same ΔV values the slope of the $\mathrm{AFC}(E_{vib})$ and $k_{ET}(E_{vib})$ dependence will be steeper when the $Q_c - Q_{LE}$ distance is large. The same conclusion may be drawn from the treatment in term of tunneling across the potential energy barrier at the surface of the adiabatic A-state: the tunneling rate depends not only on the height but also on the extension of the barrier corresponding to the energy of the initially excited level.

In the strong coupling limit, the treatment in terms of the adiabatic A-state seems to be more appropriate. In absence of the energy barrier, the optical excitation attains such a dense manifold of the vibrational levels of the A-state that the individual vibrational transitions are not resolved. We expect to observe a diffuse absorption band, the contour of which reproduces the shape of the A-state surface in the $Q \approx Q_{LE} \approx Q_g$ range. The corresponding picture in terms of diabatic LE and ionic states will be that of LE levels so strongly coupled to the quasi-continuum of the ionic state that their linewidths exceed their spacing. This means that LE state levels are depopulated at the time scale of one classical vibration period.

III. Summary of Experimental Data

As reported in part 1, the analysis of fluorescence excitation and hole-burning spectra reveals the presence of two different types of 1:1 complexes called E and R isomers. For both of them the spectra indicate the initial excitation of the $|LE\rangle$ state: in contrast to those of typical charge-transfer complexes where the ionic state is directly attained,[9] the bands are relatively narrow and only slightly red shifted with respect to the absorption of the free anthracene molecule. They differ by finer details of the excitation spectrum and by their emission:

(i) E-isomers are characterized by diffuse ($\delta\nu \approx 100-200$ cm^{-1}) absorption bands and by their exciplex-type emission, a strongly red shifted ($\Delta\nu \approx 4000$ cm^{-1}), broad ($\delta\nu \approx 3000$ cm^{-1}), structureless band with a decay time of the order of 300 ns much longer than that of anthracene (∼25 ns). This emission is the signature of a rapid A*D ⇝ A^- D^+ transfer followed by the A^- D^+ → AD emission.

(ii) R-isomers show in excitation a fine structure composed of closely spaced, narrow bands with ∼1 cm^{-1} widths. Their emission spectra depend on the excitation frequency: upon the excitation of the lowest levels they emit the resonant narrow-band A*D → AD fluorescence with a decay time close to that of anthracene. It indicates that the A*D ⇝ A^- D^+ electron transfer does not occur during the lifetime of the $|LE\rangle$ state. Upon the excitation of higher levels, the exciplex emission is observed. For each R-isomer, one can determine (or estimate) the energy threshold corresponding to the onset of the exciplex emission (i.e., of the A*D ⇝ A^- D^+ transition).

For all complexes, except for the A-DMA system, we observe multiple R-isomers while there seems to be only one E-isomer. The absence of systems with an intermediate character (resolved but significantly broadened bands) is striking.

A. Experimental Information about the A*D ⇝ A^-D^+ Relaxation Rates. The essential parameters characterizing the ET process are, for each isomer, the onset of the A^*D ⇝ A^-D^+ relaxation (i.e., of the exciplex emission) and the dependence of its rate on the vibrational energy excess E_{vib}. These onsets are listed in Table 1. The ET rates may be deduced either directly from time resolved measurements or from relative intensities of the resonant and exciplex emission components, and in the limit of a very rapid relaxation, from the homogeneous broadening of the absorption bands.

The decay times of R-isomers upon excitation of their lowest levels (below the onset of the A^*D ⇝ A^-D^+ relaxation) are nearly the same as the decay time of the bare anthracene molecule ($1/\tau_A = k_{LE} \approx 4 \times 10^7$ s^{-1}). The absence of exciplex emission for these levels implies that the ET rate is smaller than the A*D intrinsic decay rate at least by 1 order of

TABLE 1: Location of the Threshold for Observation of the Exciplex Emission for All the R-Isomers of the Complexes Studied, Determined from the Comparison of FES-R and FES-E of Each Complex

complex	threshold < 20 cm^{-1}	20 cm^{-1} < threshold < end of 0_0^0 vibrational structure	end of 0_0^0 vibrational structure < threshold < 215 cm^{-1}	end of 0_0^0vibrational structure < threshold < 385 cm^{-1}
A-DMA			R_1	
A-DMPT	R_1		R_2	
A-DMMT				R_1
				R_2
A-DMOT				R_2
				R_3
	R_4			
		R_5		
A-DEA		R_1		
		R_2		
	R_3			

magnitude. We thus have for all levels showing purely resonant emission:

$$k_{ET} \leq 5 \times 10^6\ s^{-1}$$

On the other hand, if the dual (resonant + exciplex) emission is observed, the ET rate must be of the same order of magnitude as the intrinsic decay rate of the LE state so that $5 \times 10^6\ s^{-1} < k_{ET} < 5 \times 10^8\ s^{-1}$. In this case, the ET rate may be directly deduced from the measurements of the decay rate of the resonant fluorescence compared to that of anthracene:

$$k_{ET} = 1/\tau_{res} - 1/\tau_A \quad (5)$$

For one of the isomers under study (cf. section III.B.2.iii), from the decay time reduced to ~10 ns, we deduce $k_{ET} \approx 5 \times 10^7\ s^{-1}$.

From the kinetic treatment in terms of populations N_i of LE and ionic states,

$$-dN_{LE}/dt = (k_{LE} + k_{ET})N_{LE} \quad \text{and}$$
$$-dN_{ion}/dt = (-k_{ET}N_{LE} + k_{ion}N_{ion}) \quad (6)$$

we obtain, assuming a short pulse excitation, for intensities of the resonant and exciplex emission components:

$$I_{res}(t) = k^r_{LE}N_{LE}(t) = k^r_{LE}N_{LE}(0)\exp[-(k_{LE} + k_{ET})t]$$

and

$$I_{exc}(t) = k^r_{ion}N_{ion}(t) = k^r_{ion}N_{LE}(0)(k_{ET}/k_{LE} + k_{ET}) \times \{\exp[-k_{ion}t] - \exp[-(k_{LE} + k_{ET})t]\} \quad (7)$$

hence the ratio of integrated intensities $\langle I_{res}\rangle = \int I_{res}(t)\,dt$ and $\langle I_{exc}\rangle = \int I_{exc}(t)\,dt$ will be

$$\langle I_{exc}\rangle/\langle I_{res}\rangle = (k^r_{ion}/k^r_{LE})[k_{ET}/k_{ion} - k_{ET}/(k_{LE} + k_{ET})] \quad (8)$$
$$\rightarrow (k^r_{ion}/k_{ion})/(k^r_{LE}/k_{ET}) \quad \text{when} \quad k_{ion}/k_{ET} \rightarrow 0$$

so that k_{ET} may be deduced from the intensity ratio if radiative constants and k_{ion} are known.

In systems for which only the exciplex emission is observed (the complete quenching of resonant emission), the ET rate is obviously larger than the intrinsic decay rate, hence

$$5 \times 10^8\ s^{-1} < k_{ET}$$

A direct measurement of k_{ET} in this range would necessitate picosecond light source, but the high limit of k_{ET} may be deduced from the absence of a detectable level broadening. Since in the absence of a rapid relaxation the widths of the rotational envelopes of vibronic bands in the excitation spectra of complexes are of the order of 1 cm^{-1} (cf. part 1), the homogeneous broadening of individual levels may be detected only when $\delta\nu \approx 1\ cm^{-1}$ (i.e., when $\tau \approx 5 \times 10^{-12}$ s and $k_{ET} \approx 2 \times 10^{11}\ s^{-1}$. Hence, the absence of the resonant emission and of a detectable broadening indicates

$$5 \times 10^8\ s^{-1} \leq k_{ET} \leq 10^{11}\ s^{-1}$$

while, when the broadening of absorption band is observed,

$$k_{ET} > 10^{11}\ s^{-1}$$

B. Individual Systems. In the following sections we will treat separately the E- and R-isomers.

(1) *E-Isomers.* At all excitation wavelengths, their emission is characterized by the absence of the resonant component which indicates $k_{ET} > 10^9\ s^{-1}$. This implies that no vibrational excess energy is needed for ET. The absorption bands, broad and structureless, suggest a strong homogeneous broadening due to a rapid ET process and indicates $k_{ET} \gg 10^9\ s^{-1}$.

(i) If it is supposed that the total (~150 cm^{-1}) width is homogeneous, the lifetime of the levels of the A^*D state must be as short as ~40 fs, leading to $k_{ET} \approx 2.5 \times 10^{13}\ s^{-1}$, (ii) if it is admitted that this width is inhomogeneous and results from the overlap of closely spaced individual bands (see above, II), the wash out of the vibrational structure corresponds to $\delta\nu \geq 10\ cm^{-1}$ (i.e., to the lifetimes $\tau \leq 0.5$ ps).

This leads to the following limits for the electron transfer rate:

$$2 \times 10^{12}\ s^{-1} \leq k_{ET} \leq 2 \times 10^{13}\ s^{-1}$$

The contours of bands corresponding to the 0_0^0 and X_0^n transitions involving internal modes (X) of anthracene with E_{vib} of 385 and 770 cm^{-1} are the same in the error limits which indicates a slight (if any) dependence of the ET rate on the vibrational energy contained in intramolecular modes.

(2) *R-Isomers.* The variation of ET rates with E_{vib} may be directly observed only in a limited energy range, (i.e., within the band system associated with the 0_0^0 transition of anthracene). Its extension is of the order of 90−120 cm^{-1}, and there is no absorption in the $E_{vib} > 120\ cm^{-1}$ range until the onset of the weak $\overline{11}_0^1$ vibronic transition (not observed in the spectra of weakly absorbing species) at 215 cm^{-1} or of the strong 12_0^1 transition at 385 cm^{-1}. The energy thresholds (E_{thr}) of the $A^*D \rightsquigarrow A^-D^+$ relaxation may be exactly determined only when contained in the 0− ~120 cm^{-1} limits. Otherwise, one can only show that $120 < E_{thr} < 215$ (or 385 cm^{-1}).

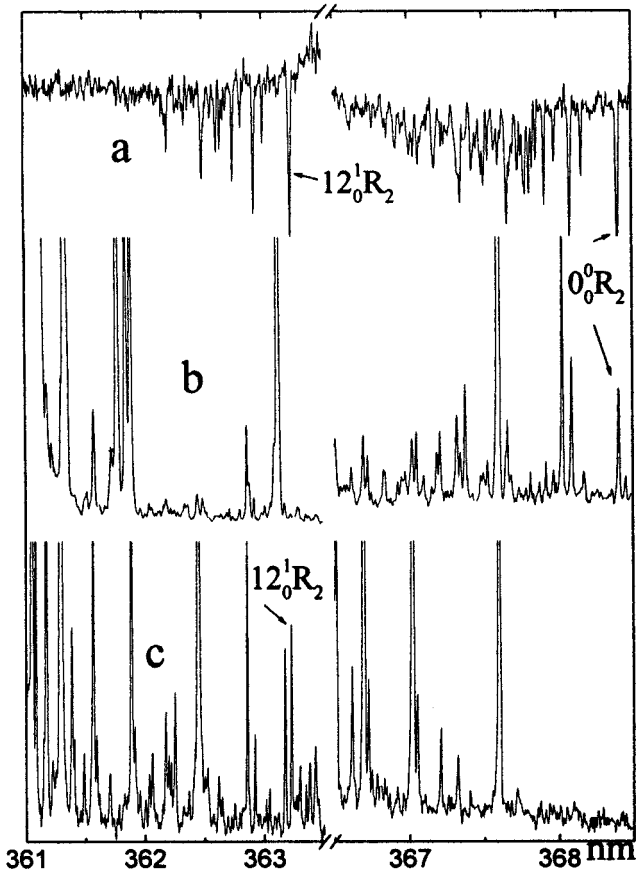

Figure 2. Spectroscopy of the R_2 isomer of the anthracene−dimethyl-*o*-toluidine complex in the 0_0^0 and the 12_0^1 range: (a) hole-burning spectrum with probe laser fixed on the 0_0^0 band and detection of the resonant fluorescence, (b) FES-R, (c) FES-E.

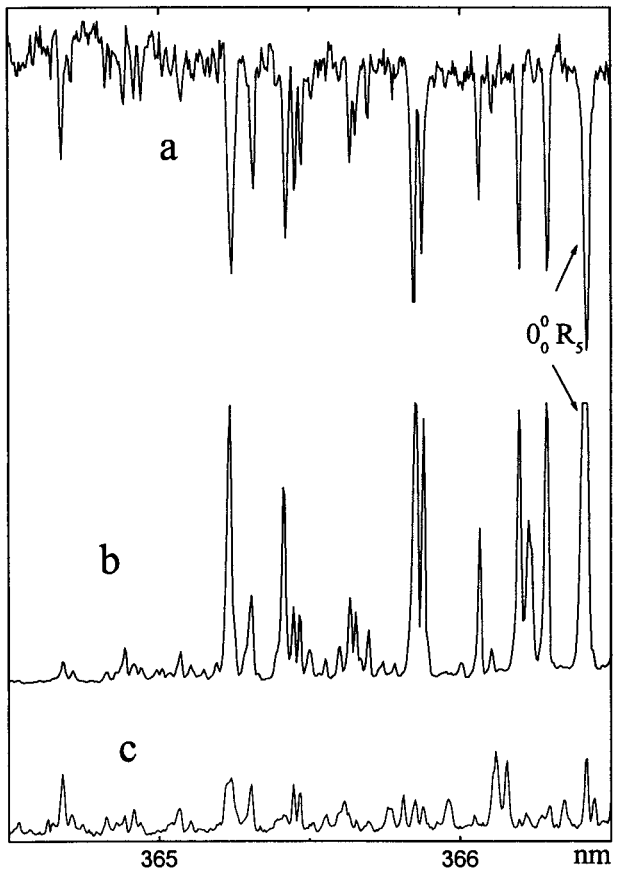

Figure 3. Spectroscopy of the R_5 isomer of the anthracene−dimethyl-*o*-toluidine complex in the 0_0^0 range: (a) hole-burning spectrum with probe laser fixed on the 0_0^0 band and detection of the resonant fluorescence, (b) FES-R, (c) FES-E.

From this point of view, one can divide all systems into three groups: (i) The onset of the $A^*D \rightsquigarrow A^-D^+$ relaxation lies between the end of the 0_0^0 band system (∼120 cm^{-1}) and 215 (385) cm^{-1}.

Most systems belong to this case (Table 1). Their characteristic feature is the absence of the exciplex emission upon excitation of any bands belonging to the 0_0^0 band system appearing in the excitation spectrum of the resonant fluorescence (FES-R). This sets the lower limit of E_{thr} above its highest levels so that $E_{thr} > 120$ cm^{-1}. On the other hand, the bands belonging to $\overline{11}_0^1$ band system (if observed) and to the 12_0^1 system are present uniquely in the excitation spectrum of the exciplex fluorescence (FES-E).

We will illustrate it by comparing the hole-burning spectra (HBS) of the R_2 isomer of the A-DMOT (Figure 2a) with the excitation spectra of the resonant and exciplex emission components (Figure 2b,c). The fluorescence from all levels of the 0_0^0 system is resonant while upon the excitation of levels belonging to the 12_0^1 system only the exciplex emission is observed. The onset of the exciplex emission lies in between.

The absence of exciplex emission for $E_{vib} < 120$ cm^{-1} indicates $k_{ET} < 5 \times 10^6$ s^{-1} while the complete quenching of the resonant emission in the absence of band broadening for $E_{vib} \geq 215$ cm^{-1} implies 10^9 $s^{-1} < k_{ET} < 10^{11}$ s^{-1}. The ET rate increases by 3 orders of magnitude or more for $\Delta E_{vib} \approx 100$ cm^{-1}. Such a rapid increase of k_{ET} is currently observed for other isomers belonging to this group.

(ii) The $A^*D \rightsquigarrow A^-D^+$ onset is located within the 0_0^0 band system (20 $cm^{-1} < E_{thr} < 120$ cm^{-1}). Only three isomers belong to this case: R_1 and R_2 of A-DEA and R_5 of A-DMOT. We illustrate this case by the R_5 isomer of A-DMOT. By comparing its HBS (a), FES-R (b), and FES-E (c), one can see that for $E_{vib} < 50$ cm^{-1} the bands are only present on the FES-R spectrum while for E_{vib} of 60−70 cm^{-1}, they appear in both FES-E and FES-R (Figure 3). We have thus $E_{thr} \approx 50-60$ cm^{-1}. The variation of the (I_{exc}/I_{res}) ratio with E_{vib} up to ∼130 cm^{-1} is plotted in Figure 4: k_{ET} increases slowly up to 100 cm^{-1} and then shows a rapid enhancement. This indicates an increase of k_{ET} by 1 order of magnitude for $\Delta E_{vib} \approx 40$ cm^{-1} (i.e., as rapid as in the previous case).

(iii) The $A^*D \rightsquigarrow A^-D^+$ relaxation appears for $E_{vib} < 20$ cm^{-1}. Three isomers belong to this group: R_4 of A-DMOT, R_1 of A-DMPT, and R_3 of A-DEA. All of them emit a dual fluorescence when excited in the origin of the 0_0^0 band system, but the dependence of their ET rates on the vibrational energy excess is different.

The spectra of the R_4 isomer of A-DMOT are represented in Figure 5. The origin band of the 0_0^0 band system appears in both FES-R and FES-E. The decay of the resonant emission is long enough to enable direct measurements of its lifetime found equal to ∼10 ns, significantly shorter than that of other isomers showing only the resonant emission ($\tau \approx 20$ ns). From eq 5, we deduce $k_{ET} \approx 5 \times 10^7$ s^{-1}. For higher levels of the 0_0^0 band system, the intensity ratio $\langle I_{exc} \rangle / \langle I_{res} \rangle$ increases slowly with E_{vib}, but this ratio is much larger for a few levels (Figure 6) suggesting that the ET rate depends not only on the overall energy but is mode selective. This problem will be discussed in V.B.

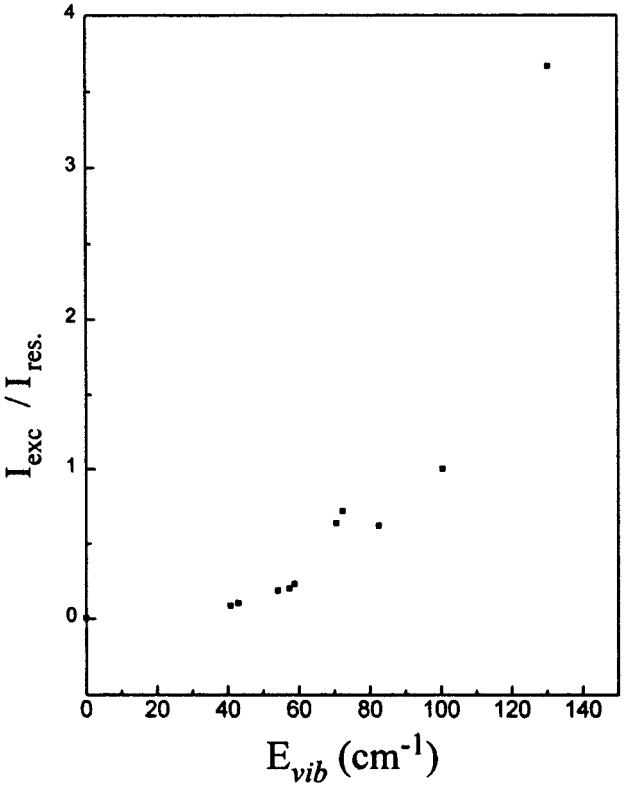

Figure 4. Dependance of the I_{exc}/I_{res} ratio on E_{vib} for the R_5 isomer of the anthracene−dimethyl-*o*-toluidine complex.

The behavior of the isomer R_3 of A-DEA is similar: a dual emission is observed only for the four lowest levels ($E_{vib} < 25$ cm^{-1}) with rapidly varying $\langle I_{exc}\rangle/\langle I_{res}\rangle$ ratio, while from the higher levels ($E_{vib} > 25$ cm^{-1}) only the exciplex fluorescence is emitted. In contrast to it, for the R_1 isomer of A-DMPT, the dual emission is limited to the origin of the 0_0^0 band system and the emission from the next level ($E_{vib} = 18$ cm^{-1}) is already of exciplex type.

Upon the excitation of bands (excitation of higher ($E_{vib} \geq 385$ cm^{-1}) levels) belonging to the vibronic transitions ($12_0^1 = 0_0^0 + 385$ cm^{-1}, $12_0^2 = 0_0^0 + 770$ cm^{-1}, etc.) of all complexes under study, the emission spectrum corresponds to the exciplex fluorescence, the resonant emission being completely quenched. We do not observe, however, any significant broadening of bands which would indicate an enhancement of k_{ET} above the 10^{11} s^{-1} threshold. It suggests that the energy contained in intramolecular modes does not induce a significant acceleration of the ET process (cf. V).

The only exception to this rule is the R_1 isomer of the A-DMOT complex showing the resonant emission from the levels of the 0_0^0 band system but no emission from those belonging to the 12_0^1 group. In this case we observe a significant broadening of the 12_0^1 bands in the HB spectra which suggests the opening of an additional, efficient relaxation channel for the energy excess above the 130 cm^{-1} limit (resonance with a triplet level enhancing the intersystem crossing rate ?).

IV. Modeling

In order to explain the mechanism of the ET reaction, the knowledge about the PESs of the excited states of complexes is necessary. These calculations are performed for both diabatic states |LE⟩ and |ion⟩ of all complexes excepted that of DEA. The most relevant parameters are (i) positions and depths of the energy minima, (ii) positions and heights of the energy barriers, (iii) the crossing area between LE and ionic surfaces

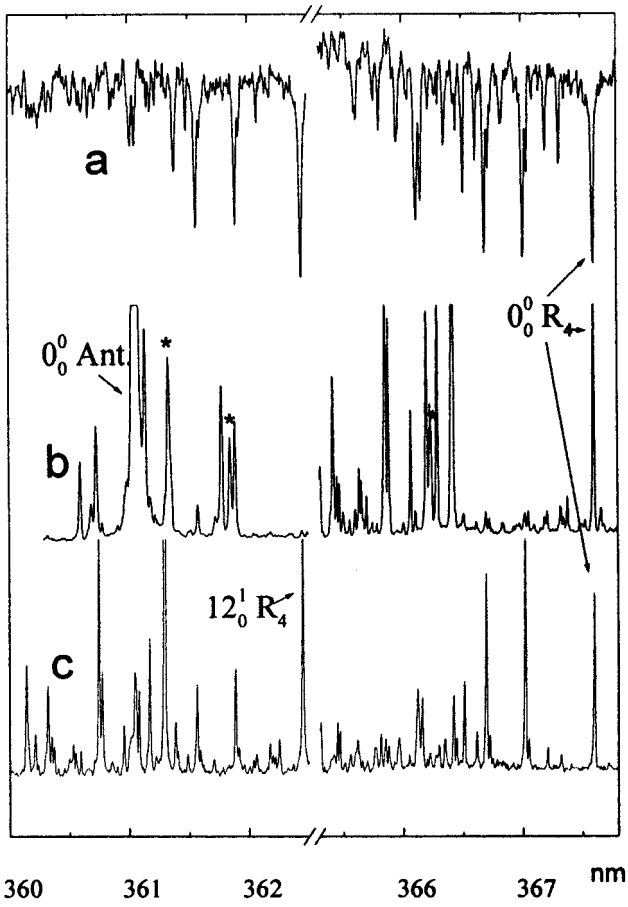

Figure 5. Spectroscopy of the R_4 isomer of the anthracene−dimethyl-*o*-toluidine complex in the 0_0^0 and the 12_0^1 range: (a) hole-burning spectrum with probe laser fixed on the 0_0^0 band and detection of the resonant fluorescence, (b) FES-R, (c) FES-E.

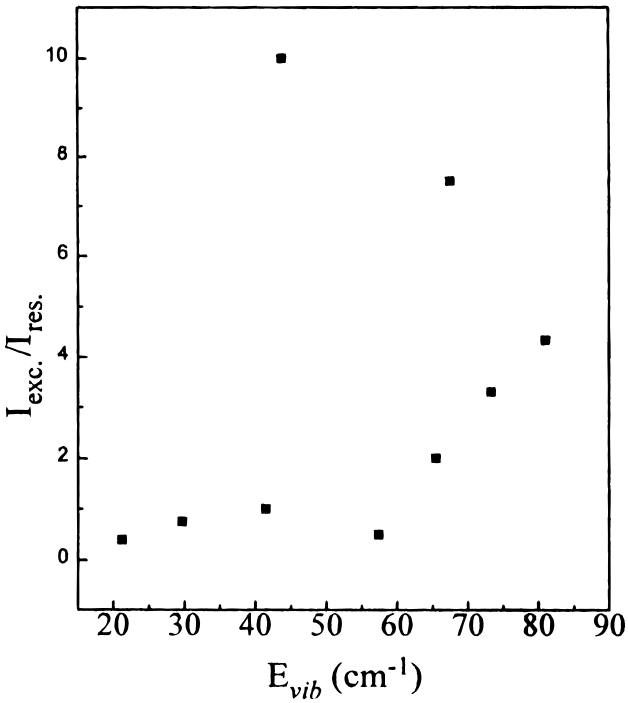

Figure 6. Dependence of the I_{exc}/I_{res} ratio on E_{vib} for the R_4 isomer of the anthracene−dimethyl-*o*-toluidine complex.

energetically accessible from the minima of the LE state, and (iv) the LE−ion coupling strength in the crossing area.

A. Calculation Techniques and Approximations. The calculations of PES of the locally excited and ionic states were carried out using the same techniques as those used for the ground-state surface and described in part 1. The changes of the molecular structures and properties induced by excitation or ionization must be taken into account: (i) we assumed that the geometry of anthracene in the $|LE\rangle$ and $|ion\rangle$ state is the same as that in its ground state. We supposed that the structure of the aniline derivatives is unchanged in the LE state. We were looking for the crossing of LE and ionic surfaces for identical (nonplanar) structures of the donor in A*D and A^-D^+ species. On the other hand, the calculations of the A^--DMA^+ energy minimum were carried out for the DMA^+ ion with the dimethylamino group in the ring plane. Their results are valid also for DMPT and DMMT complexes.

(ii) The distribution of the electric multipoles in the excited anthracene molecule was determined by CI calculations taking into account all monoexcited configurations. Similar calculations were performed for A^- and D^+ ions by an open-shell UHF-SCF treatment. One can thus consider that electrostatic terms are obtained with the same accuracy as for the ground state complexes.

(iii) The major problem is the lack of information about the polarizibilities of excited molecules and ions. The dispersion and polarization terms were thus computed using the same parameters as for the ground state molecules. Since the polarizibility is usually enhanced by electronic excitation, both terms are underestimated. In the case of the ionic state, the polarizibility of the A^- ion is larger and that of D^+ smaller than those of neutral A and D molecules so that errors partially compensate each other.

The intersection of the PESs of the LE and ionic states in the vicinity of each minimum of the LE surface was localized using the Monte Carlo method. The part of the LE surface with energies lower than that of the lowest saddle point delimiting the basin was explored. Energies of LE and ionic states were calculated at each point in order to check whether two PES's cross (or at least approach closely one to the other) within the attraction basin corresponding to a given minimum. The configurations at the crossing area are determined in this way.

In order to estimate the configuration dependence of the $H_{LE,ion}(Q)$ coupling matrix element, supposed to be proportional to S_{AD}, the overlap integral S_{AD} between the HOMO's of A and D, we calculated S_{AD} for relevant configurations of the donor-acceptor pair.

B. Results. The calculated geometry and relative energies of the energy minima as well as positions and energies of the saddle points at the LE state surface are nearly the same as in the ground electronic state. Our calculations do not reproduce the observed red shift of ∼500 cm^{-1} (∼1.5 kcal/mol) of the AD → A*D transition with respect to the A → A* transition in the bare anthracene molecule . This discrepancy is obviously due to the underestimation of the dispersion term. Since this term is relatively insensitive to the mutual orientation of molecules, one can suppose that the error may be corrected by a shift of the whole LE state surface to lower energies. This picture is consistent with the experimental data showing that (i) the equilibrium configurations of the *i*th isomer in its ground and LE state are nearly the same $Q_{LE}(i) \approx Q_g(i)$, as evidenced by the intensity distribution within the fine structure of the 0_0^0 band systems (short progressions with the maximum in the origin band) and (ii) the energy differences $V_A(Q(i)) - V_g(Q(i))$

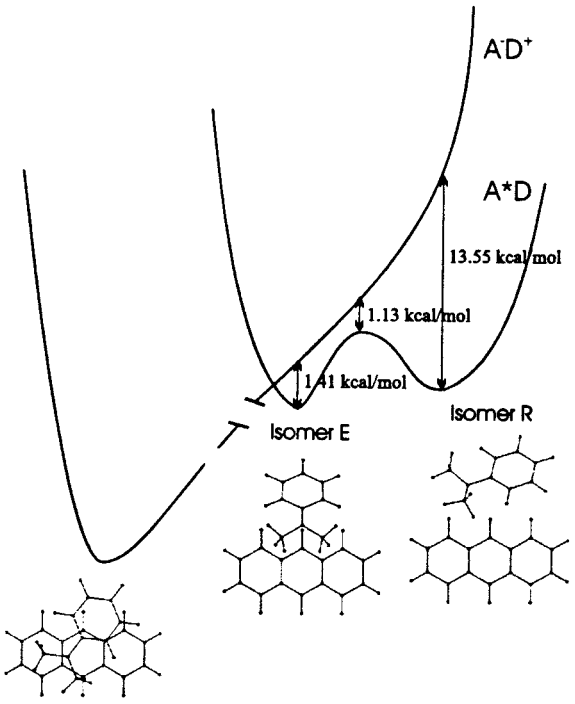

Figure 7. Structures of two principal isomers of the anthracene dimethylaniline complex and that corresponding to the minimum of the ionic surface obtained by the Claverie method and schematic representation of the LE and ionic surfaces in the vicinity of their crossing.

(i.e., red shifts observed for different R-isomers) of the same complex are only slightly different from one another with the only exception of the A-DMOT complex.

For the ionic state of all complexes except that of DMOT the calculations indicate a single minimum with a stacked structure and the distance between the ring planes reduced to 3.25 Å (Figure 7). The $-NR_2$ group (contained in the ring plane) is situated above the central anthracene ring and the energy depends only slightly on the angle between the long axis of the donor and the short axis of the acceptor in the $\langle -\pi/4, \pi/4\rangle$ limits.

The accuracy of this calculation may be checked by comparing the calculated energy difference between this minimum and the corresponding point on the ground state surface: $V_{ion}(Q_{ion}) - V_g(Q_{ion})$ with the frequency of the exciplex emission $A^- D^+ \rightarrow AD$. The calculated energy is overestimated by ∼1600 cm^{-1} (∼4.6 kcal/mol) for all complexes except that of DMOT for which this difference is more important (∼8.6 kcal/mol). This error, not exceeding 5% of the total binding energy, is probably due to underestimation of dispersion and polarization terms, as in the case of the LE state. These energy corrections do not deeply modify the picture of the surface crossing: in view of the shallow shape of the LE surface and the very steep decrease of the ionic state energy in the crossing region, the crossing area is not sensitive to a few kilocalorie shifts of diabatic surfaces (Table 2).

The equilibrium configuration of $A^-(DMOT)^+$ is different: T-shaped with the $-NR_2$ approaching closely the central ring of anthracene. The energies of the secondary minima with structures close to the stacked one are higher by ca. 4 and 7 kcal/mol. The reason for this difference is an exceptionally high value of electrostatic and polarization terms due to a large value of positive charge localized at the N-atom, the NR_2−ring conjugation being practically suppressed by the steric hindrance effects.

TABLE 2: Variation of the Energy Position of the Lowest Crossing Point Between AD and A^- D^+ States as a Function of the Energy Shift of the A^- D^+ PES for the Anthracene−Dimethylaniline Complex[a]

shift of A^-D^+ PES (in kcal/mol)	4.60	3.60	2.60	1.60
energy of the lowest crossing point (in kcal/mol) relative to A + D at d(A−D) = ∞	73.89	73.95	73.98	74.06
energy shift of the lowest crossing point relatively to the bottom of the minimum 1 well (in cm^{-1})	7	28	40	67

[a]Similar results were obtained in the case of the anthracene−dimethyl-*p*-toluidine and anthracene−dimethyl-*m*-toluidine complexes.

Complete results for different complexes are represented in Figure 8. For each complex are given (i) the energies (V_i) of the main energy minima in the LE state, the energy of the deepest one being taken as zero, the minima are numbered as in part 1 and their configurations Q_i are nearly the same as in the ground electronic state (cf. part 1), (ii) the energies of the ionic state (I_i) for each Q_i configuration, (iii) the energies of the saddle points between the minima *i* and *j* at the LE surface (V_{ij}), and (iv) the energies (V_{ic}) of the lowest crossing point of LE and ionic surfaces in the vicinity of *i*th minimum (if this energy is lower than the lowest V_{ij}).

These schemes enable us to predict the pathways followed by the molecular systems prepared by optical excitation in the vicinity of each minimum with a given vibrational energy content.

The calculated values of the S_{AD} overlap integral are only slightly dependent on the complex configuration in the relevant configuration range varying for the DMA complex from 3.7×10^{-3} for minimum (1) to 4×10^{-3} for minimum (2) and to 5×10^{-3} for the 1-2 saddle point. One can thus admit that the coupling constant $H_{LE,ion}(Q)$, equal to $\sim 20 S_{AD}$,[2] is of the order of 800 cm^{-1} (∼2 kcal/mol) in the whole range. This value is close to that deduced from experiment for other systems of this kind.[9,10]

It must be kept in mind that in a nonnegligible fraction of the configuration space the energy difference $|V_{ion}(Q) - V_{LE}(Q)|$ and $H_{LE,ion}(Q)$ are of the same order of magnitude. The surface of the A-state may thus be significantly different from those of LE and ionic state surfaces. The energy of the A-state at Q_c is reduced by $\delta V_i = H_{LE,ion}(Q_c)$ but the V_{ij} barrier on the LE surface will be also lowered by

$$\delta V_{ij} = {}^1/_2\{|V_{ion}(Q_{ij}) - V_{LE}(Q_{ij})|^2 + 4[H_{LE,ion}(Q_{ij})]^2\}^{1/2} - {}^1/_2|V_{ion}(Q_{ij}) - V_{LE}(Q_{ij})|$$

and some *i*−*j* barriers may be even suppressed.

V. Discussion

A. Mechanism of the Electron Transfer. Using the Figure 8a−d, we will try to identify the energy minima corresponding to E-isomers denoted as configurations Q_E and those of R-isomers (configurations Q_R).

(1) *E-Isomers.* The spectra of E isomers indicate the electron transfer taking place at the subpicosecond time scale. This suggests that the energy barrier at the A-state surface between the initial ($Q \approx Q_E$ with the energy $V_A(Q_E) \approx V_{LE}(Q_E)$ and wave function $|A(Q_E)\rangle \approx |LE\rangle$) and final configuration ($Q \approx Q_{ion}$, $V_A(Q_{ion}) \approx V_{ion}(Q_{ion})$, $|A(Q_{ion})\rangle \approx |ion\rangle$) is negligible or absent. This absence (strong coupling limit) implies following conditions for the diabatic states for which our calculations are performed: (i) the potential energy in the crossing point Q_c of the LE and ionic surfaces $V_{LE}(Q_c) = V_{ion}(Q_c)$ is not much higher than $V_{LE}(Q_E)$, (ii) this energy difference $\Delta V = V_{LE}(Q_c) - V_{LE}(Q_E)$ is equal or smaller than $H_{LE,ion}(Q_c)$ in the crossing region (∼2 kcal/mol), and (iii) the geometries Q_c, Q_E, and Q_{ion} are not very different so that not only the height but also the extension of the energy barrier is not too large. This condition may be formulated in a somewhat different way: the evolution from Q_E to Q_{ion} does not necessitate an important change of more than one external coordinate.

For DMA, DMPT, and DMMT complexes, these conditions are fulfilled for the configuration (1) $Q = Q_1$. In A-DMA, the energy gap between ionic and LE surfaces at $Q = Q_1$ is of 1.80 kcal/mol so that $V_{ion}(Q_1) - V_{LE}(Q_1) \approx H_{LE,ion}(Q)$ and the two states are strongly mixed. Moreover, $\Delta V = V(Q_c) - V_{LE}(Q_E) \approx 0.02$ kcal/mol, so that the A-surface is obviously barrierless. The values obtained for the two other complexes (Figure 8b,c) are nearly the same. The structure Q_1 is also similar to that of the equilibrium configuration of the ionic state: by rotation of the donor molecule around its short axis we attain the geometry with parallel molecular planes and the NR_2 group in a close contact with the acceptor π-electron system. Note that for the minima (2) of the three complexes, the energy gaps calculated in the same way are respectively 13.55, 12.51, and 13.42 kcal/mol and their geometries are quite different from those of the ionic state. We may thus assume that the minimum (1) of all three complexes corresponds to the E-isomer. Since the minimum (1) is the deepest one in the ground electronic state and shows a high occurrence, this assignment is compatible with a high relative intensity of the E isomer bands in the fluorescence excitation spectra of A-DMA, A-DMPT, and A-DMMT complexes. This assignment is probably valid also for A-DEA.

The case of A-DMOT complex is different. The configuration close to that of ionic state is that of the minimum (4) with the energy gap between ionic and LE states of the order of 1 kcal/mol, while it amounts to ∼6.63 and ∼16.61 kcal/mol for deep minima (1) and (2). The E-isomer corresponds in this case to a relatively weakly bound form (its interaction energy is of -4.06 as compared to -5.11 kcal/mol for the form (1) and its occurrence is also lower). This is probably the reason why the relative population of the E-isomer is much smaller in the spectrum of A-DMOT than in the spectra of all other complexes (cf. part 1).

(2) *R-Isomers.* All other minima are assigned to R-isomers showing the energy threshold for ET in the $E_{vib} = 0-400$ cm^{-1} range with the maximum value of k_{ET} not exceeding 10^{11} s^{-1} for their highest levels. This value is smaller by a factor of 20 or more as compared to the ET rates of E-isomer. Such a gap indicates a qualitative difference between the ET mechanisms in the case of R and E isomers. Two possible mechanisms must be taken into account: (i) a direct R ⇝ ion transition analogue of that observed for E-isomers but with a nonzero energy threshold and a strongly reduced above-threshold rate and (ii) a sequential R ⇝ E ion process involving as the first and rate-determining step an isomerization at the LE energy surface followed by a rapid crossing to the ionic state.

The actually available experimental data do not allow us to exclude one of these two pathways but strong arguments in favor of the second one may be deduced from calculations.

(i) We explored by the Monte Carlo method (cf. IV) the basins corresponding to each energy minimum of the LE state surface assigned to an R-isomer. As shown in Figure 8a−d, we did not find for most of them any crossing between LE and

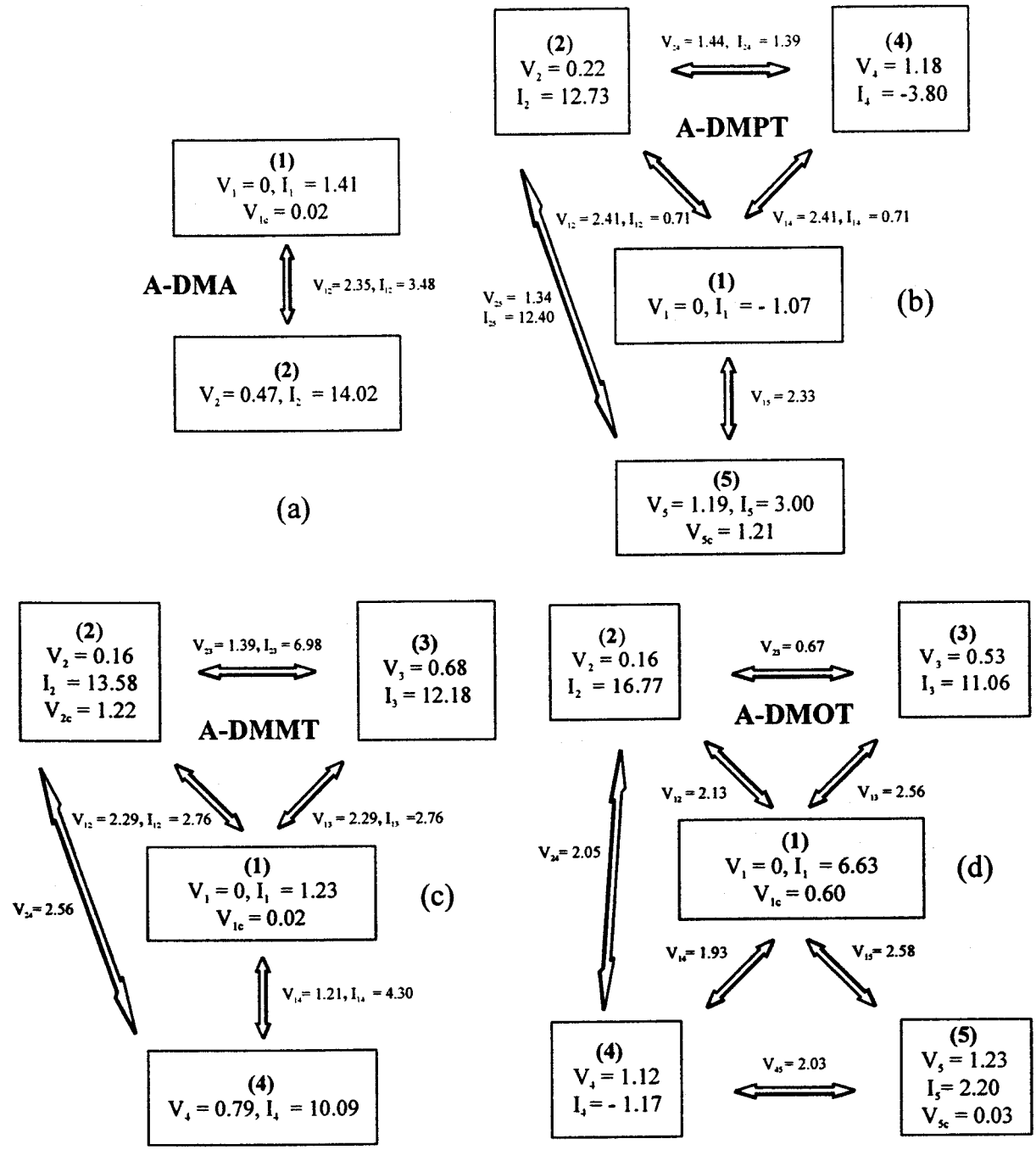

Figure 8. Summary of the results of the modeling of the LE and ionic PES's for all complexes, in each scheme a−d are given (i) the energies (V_i) of the main energy minima in the LE state, the energy of the deepest one being taken as zero. The minima are numbered as in part 1, (ii) the energies of the saddle points between the minima *i* and *j* at the LE surface (V_{ij}), (iii) the energies (V_{ic}) of the lowest crossing point of LE and ionic surfaces in the vicinity of *i*th minimum (if this energy is lower than the lowest V_{ij}), (iv) the energies of the ionic state (I_i) are given for each Q_i and $Q_{i,j}$ configuration. For these complexes, the absolute energy of the deepest minima and the absolute energy of the ionic PES minimum (relative to A + D with $d_{AD} = \infty$) are respectively A-DMA 73.90, 64.08; A-DMPT 73.88, 61.05; A-DMMT 73.67, 62.90; and A-DMOT 74.04, 65.61. All energies are expressed in kcal/mol.

ionic surfaces at the relative energies lower than that of the lowest saddle point separating this minimum from other minima at the LE surface. The barriers separating different LE-type minima (respectively R→ E and R→ R) are less sensitive to the LE−ion coupling than in the case of crossing points between LE and ion surfaces but may be also significantly lowered. This is the case of the barrier separating the minimum (2) assigned to the R-form from the minimum (1) corresponding to the E form at the LE surface of the A-DMA complex. As shown in Figure 7, the energy gap between the LE and ion PES's for the minimum 1 and the saddle point between minima 2 and 1, is one order of magnitude lower than that corresponding to the minimum 2. This results, at the A-state surface, in a lowering of minimum (1) and saddle point energies while energy of minimum (2) is only slightly modified. Note also that the configuration corresponding to the saddle point is more similar to that of minimum (2) than to that of minimum (1). This explains that for this complex the calculated barrier between minima (2) and (1) at the A-state surface will be lowered and will become of the same order of magnitude as the observed ET threshold of $120 \leq E_{thr} \leq 215$ cm^{-1} (this is also valid for the A-DMPT and A-DMMT complexes).

(ii) The ET rate from high (well above the ET threshold) levels of the R-isomers are much lower than those of E-isomers. Within the model assuming a direct R → ion transition, this difference may be explained only by the values of the $H_{LE,ion}(Q)$ coupling constant much lower in the case of R−ion intersection than in that of the E−ion crossing. This explanation is, however, not compatible with the slight dependence of S_{DA}, (i.e., of H_{LE-ion}) on complex configuration.

We prefer, therefore, to assume a sequential mechanism for ionization of the R isomers with a slow isomerization at the LE surface as the rate determining step. This assumption of a process involving heavy particles is consistent with strongly reduced ET rates.

B. Energy Dependence of the ET Rates of R-Isomers. As previously discussed (II.), the ET rates increase rapidly with the vibrational energy excess E_{vib}. The slope of the $k_{ET} = f(E_{vib})$ is for this group of systems larger than in the case of most other AD complexes[12] and A−B−D bridged bichromophoric molecules.[13] Such a behavior corresponds to systems with relatively low but extended energy barriers. As a matter of fact, the configurations of minima (1) and (2) assigned to R and E isomers are situated far from one another at the LE-state surface. The probability of the 2 → 1 transition increases rapidly with E_{vib} but remains low even for $E_{vib} > V_{12}$.

The energy dependence of the ET rates may be followed in a more detailed way for the isomeric forms with the ET thresholds at $E_{vib} < 120$ cm^{-1} (i.e., the 0_0^0 band system, the whole vibrational energy being injected into external modes ($E_{vib} = E_{ext}$). One can then check whether the ET rate is a simple function of E_{vib} or depends also on the specific properties of the initially excited mode. From a limited number of observations one can tentatively deduce the following rule : the ET rate depends on the excited mode only for $E_{vib} < 50$ cm^{-1} and varies monotonically with energy above this limit. This behavior may be correlated with a typical value of the IVR threshold for molecular complexes of this size, of the order of 70 cm^{-1} for perylene−anisole[11] and perylene−benzene[14] complexes. For the lowest levels, IVR is absent or so slow that electron transfer takes place from the initially excited level and may be mode sensitive. Above the IVR threshold, the energy is redistributed with a rate of $10^{10}-10^{11}$ s^{-1} before ET occurs. The observed ET rate is an average value for a whole set of levels with the same overall energy and is independent of the initially excited mode.

The case of levels belonging to vibronic X_0^n transitions involving internal modes of anthracene is similar. Their initial vibrational energy is the sum of energies contained in internal and external modes: $E_{vib} = E_{int} + E_{ext}$ and typically $E_{int} > E_{ext}$ (e.g., for the 12_0^2 transition in A-DMA we have $E_{int} = 770$ cm^{-1} and $E_{ext} \leq 100$ cm^{-1}). It is interesting to note that such a large amount of energy in internal modes does not induce a significant line broadening. This suggests that this part of energy has no influence on the rate of the R → E isomerization as long as this energy is not redistributed between external modes.

One can thus consider that the X^n levels decay by two pathways: (i) isomerization (ET) with a rate dependent only on E_{ext} (i.e., the same as in the case of the 0_0^0 band system) (ii) a rapid IVR followed by the R → E isomerization from the levels with $E'_{int} = 0$ and a large amount of energy in external modes ($E'_{ext} = E_{int} + E_{ext}$). This second step is probably very rapid but the overall ET rate is determined by the rate of IVR from internal to external modes.

VI. Conclusions

The irreversible $A^*D \rightarrow A^-D^+$ electron transfer was observed for all complexes studied here but the energy thresholds and rates of this process are strikingly different for different complexes and different isomeric forms of the same complex. The difference between the E-isomers with $k_{ET} > 2.10^{12}$ s^{-1} and R-isomers with $k_{ET} = 10^6-10^{11}$ s^{-1} in absence of intermediate forms may be rationalized by assuming different mechanisms in both cases: a direct electron transfer in the first and the sequential process in the latter one with the R → E isomerization as the first, rate-determining step.

The electron transfer in isolated molecular systems may be treated in terms of the theory of nonradiative transitions either as electronic relaxation between diabatic LE and ionic states or as an evolution at the single energy surface of the adiabatic A-state. The first picture seems to be the best in the case of a weak LE−ion coupling (R-isomers) and the second one in that of a strong coupling in E-isomers.

We tentatively assigned the equilibrium configurations deduced from modeling of energy surfaces which correspond to the most abundant R an E species. They do not correspond to simple (stacked or T-shaped) structures.

The most important conclusion is the extreme sensitivity of the ET rates to the mutual orientation of donor and acceptor molecules forming different complexes with nearly the same intermolecular distances close to the sum of van der Waals radii. This result suggests that also in condensed phases the probability of electron transfer depends not only on the intermolecular distance but also on the angular coordinates of the donor−acceptor pair.

References and Notes

(1) Beens, H.; Knibbe, H.; Weller, A. *J. Chem. Phys.* **1967**, *47*, 1183.
(2) Knibbe, H.; Röllig, K.; Schäfer, F. P.; Weller, A. *J. Chem. Phys.* **1967**, *47*, 1184.
(3) Saigusa, H.; Itoh, M. *Chem. Phys. Lett.* **1984**, *106*, 391.
(4) Anner, O.; Haas, Y. *Chem. Phys. Lett.* **1985**, *119*, 199.
(5) Chakraborty, T.; Lim, E. C. *Chem. Phys. Lett.* **1994**, *230*, 137.
(6) Brenner, V.; Millié, P.; Piuzzi, F.; Tramer, A. *J. Chem. Soc., Faraday Trans.* **1997**, *93*, 3277.
(7) Bixon, M.; Jortner, J. *J. Phys. Chem.* **1993**, *97*, 13061.
(8) Deperasinska, I.; Prochorow, J. *Chem. Phys. Lett.* **1989**, *163*, 257.
(9) Russell, T. D.; Levy, D. H. *J. Phys. Chem.* **1982**, *86*, 2718.
(10) Amirav, A.; Castella, M.; Piuzzi, F.; Tramer, A. *J. Phys. Chem.* **1988**, *92*, 5500.
(11) Castella, M.; Millié, P.; Piuzzi, F.; Caillet, J.; Langlet, J.; Claverie, P.; Tramer, A. *J. Phys. Chem.* **1989**, *93*, 3949.
(12) Saigusa, H.; Itoh, M.; Baba, M.; Hanazaki, I. *J. Chem. Phys.* **1987**, *86*, 2588.
(13) (a) Syage, J. A.; Felker, P. M.; Zewail, A. H. *J. Chem. Phys.* **1984**, *81*, 2233. (b) Kurono, M.; Takasu, R.; Itoh, M. *J. Phys. Chem.* **1995**, *99*, 9668.
(14) Motyka, A. L.; Wittmeyer, S. A.; Babitt, R. J.; Topp, M. R. *J. Chem. Phys.* **1988**, *89*, 4586.